BUTTERWORTH HEINEMANN

*Polymer* Vol. 36 No. 12, pp. 2379–2387, 1995

0032-3861/95/$10.00+0.00

# Accelerated physical ageing of thin glassy polymer films: evidence from gas transport measurements

**P. H. Pfromm* and W. J. Koros†**

*Department of Chemical Engineering, The University of Texas at Austin, Austin, TX 78712, USA*

*(Received 1 May 1994; revised 28 October 1994)*

Single-gas permeabilities, selectivities and activation energies of permeation of thin (~0.5 μm), intermediate and thick (~25 μm) amorphous glassy polymer films of a polysulfone (Udel 1700) and a polyimide (6FDA–IPDA) were investigated. The films had identical thermal histories and were solvent-free. Evidence of strongly thickness-dependent physical ageing was discovered. Thin films showed decreasing permeabilities and increasing selectivities that surpassed those of intermediate and thick films. Thin films showed increased activation energies of permeation. These results provide evidence for an accelerated approach of thin films to the densified equilibrium state.

**(Keywords: thin films; ageing; gas separation)**

## INTRODUCTION

Thin membranes (of several hundred to several thousand ångströms thickness) made from glassy polymers are important for gas separations by membrane permeation[1–3]. Physical ageing of glassy polymers is a well known phenomenon[4–6]. It is the purpose of this paper to document physical ageing of thin (~5000 Å = 0.5 μm) and thick (~25 μm) glassy polymer films far below the glass transition temperature $T_g$. According to our results, ageing apparently proceeds much faster in the thin polymer films with a thickness characteristic of gas separation membranes than in thick films. This paper deals with the influence of this apparent accelerated ageing on the gas transport properties.

Although the vast majority of work on ageing of glassy polymers has been carried out on samples that are significantly thicker than the active layer of gas separation membranes, some studies have considered ageing of samples with comparable geometry.

Braun and Kovacs[7] have studied the volume recovery of glassy polystyrene samples in the form of moulded sheets (thickness 1 mm) and a fibrous powder (thickness 0.1 to 1 μm). This is one of the few examples of a direct comparison of thin and thick samples. Only the data for dilatometry in virtually non-sorbing organic liquids and mercury are of interest here, since highly sorbing liquids may influence the results. Physical ageing was studied down to 20°C below $T_g$ for about 100 h. The authors concluded that no significant differences were found for thin and thick samples. Braun and Kovacs' work differs greatly from the work presented here. In the present case, the temperature was at least 150°C below $T_g$ and ageing was observed over several thousand hours via gas permeation property probes.

The work on sorption in small polymer spheres appears to be the most extensive, with a geometry that is comparable to thin films[8–10]. For the most part, non-Fickian kinetics and swelling-induced effects were the focus of these studies.

Evidence of peculiarities in permeation properties of gas separation membranes with thin skins has been reported[11–15] for integral-asymmetric structures and composites formed from a wide variety of glassy polymers. The apparent active thickness ranged from as low as a few hundred ångströms to several thousand ångströms. The experimental results can be summarized as follows:

(1) Pressure-normalized gas fluxes of thin-skinned composite and integral-asymmetric membranes often decrease significantly with time.

(2) Simultaneous with the flux reductions, gas selectivities increase with time and *exceed* the values for thick films made from the same materials.

(3) The activation energies of permeation are often higher for thin-skinned membranes than for thick reference films.

The interpretation of these results is complicated by the differences in thermal and mechanical history of the membranes and thick reference films. A strong history dependence is, indeed, one of the intriguing features of glassy polymers. In addition, doubts are not easily removed that residual solvents and mechanical tension may be partly responsible for the observed effects in thin-skinned gas separation membranes.

It has been hypothesized that physical ageing of glassy polymers may show a thickness dependence, resulting in accelerated densification of thin polymer films. Alfrey and co-workers[16] suggested a diffusive removal of free volume

* Present address: Institute of Paper Science and Technology, 500 10th Street NW, Atlanta, GA 30318, USA
† To whom correspondence should be addressed

from the glassy material. They concluded that a strong thickness dependence should then be found, somewhat akin to the diffusive removal of penetrant molecules from a glassy polymer. Adopting this hypothesis, the effects observed in thin gas separation membranes could be rationalized, since ageing and the concurrent densification in general may decrease permeabilities and increase selectivities. Some experimental evidence of accelerated ageing in thin glassy films will be discussed below.

Bogdanova *et al.*[17] investigated thin crosslinked epoxide polymer films formed on various substrates. The densities of the thin films increased with time and were found to be higher than those of thick films. The authors suggest a diffusion mechanism for the elimination of free volume that is important in films of 800 $\mu$m or less. This thickness-dependent diffusion mechanism would act in addition to the well known bulk relaxation mechanisms observed in thick samples.

It is well known that the elimination of lattice disturbances in thin metal films, as opposed to thick films, takes place rapidly, even at room temperature[18]. Diffusion and condensation of vacancies as well as elimination of lattice disturbances at the sample surface have been theoretically described and experimentally confirmed.

Phase separation in free (unsupported) aluminium–copper alloy films with thicknesses of 1000–2000 Å showed that the rapid quenching of these thin films led to amorphous materials with a much lower number of quenched-in vacancies than was expected for bulk materials[19,20]. The authors attribute this to the action of the surface as a sink for existing vacancies. Certain phase separation phenomena that the authors observed in thick films do not occur in thin films denuded of vacancies.

Spaepen[21] investigated the behaviour of defects in metallic glasses. The author shows that a vacancy in an amorphous body made up of hard spheres will be partially eliminated at the surface through special sites with long-range elastic strain fields. It seems possible that the probability of such strain fields in contact with the sample surface is increased in very thin structures.

The rearrangement processes in metal films are of course very fast when compared to glassy polymer films, since the geometrical restrictions of long polymer chains are not present. However, these results clearly point to the possibility of thickness-dependent ageing of glassy polymer films.

In our work, thin, intermediate and thick glassy polymer films were investigated. The history of the films was carefully controlled, with the goal of obtaining samples that differed only in their thickness. The effect of physical ageing was examined far below $T_g$ by gas transport measurements. Our results strongly support the hypothesis of accelerated physical ageing in thin glassy polymer films, causing significant time dependences of the gas transport properties that are not observed in thick films.

## THEORY

The steady-state permeation of single gases of high purity was investigated. The temperature range was moderate, between about 20 and 50°C. Since it was the purpose to use gas transport properties as a tool to investigate physical ageing and its thickness dependence, care was taken not to alter the properties of the polymer by significant swelling or conditioning of the sample. The samples were contacted only with He, $N_2$ and $O_2$ at moderate temperatures and pressures.

The steady-state permeation flux of a single gas through a polymer film (one-dimensional diffusion) is given by Fick's first law according to:

$$N = -D(\partial C/\partial x) \tag{1}$$

where $D$ is the diffusion coefficient, $C$ is the local penetrant concentration in the film and $x$ refers to the film thickness ($x=0$ upstream, $x=l$ downstream). The driving force $(\partial C/\partial x)$ can be replaced by the pressure difference $\Delta p$, if Henry's law is assumed to apply. For the measurements performed in this work, a constant diffusion coefficient $D$ is a good approximation. A permeability coefficient can be defined as:

$$P \equiv N/(\Delta p/l) \tag{2}$$

The thickness $l$ of the film is given in centimetres (cm) and the driving force is the penetrant pressure difference $\Delta p$ across the film in centimetres of mercury (cmHg). $P$ is the steady-state permeability coefficient, usually given in Barrers ($1\ \text{Barrer} = 10^{-10}\ \text{cm}^3\text{(STP)}\ \text{cm/cm}^2\ \text{cmHg s}$). The driving force $\Delta p$ can be replaced by the upstream pressure $p$ since the downstream pressure was always kept negligible. By combining equation (1) with a constant diffusion coefficient, equation (2), and assuming Henry's law applies, one obtains[22]:

$$P = DS \tag{3}$$

where $S$ is the solubility coefficient ($\text{cm}^3$ gas (STP)/$\text{cm}^3$ polymer cmHg). The diffusion coefficient $D$ for a gas in the system of a polymer and a small amount of penetrant gas is generally accepted to depend in some form on the free volume in the system and is expected to decrease with decreasing free volume[4]. Since the free volume in a glassy polymer depends on the history of the sample, a similar dependence is to be expected for $D$.

For a glassy amorphous polymer, the solubility coefficient $S$ will depend on the penetrant pressure and Henry's law generally does not apply, except at very low pressures[23]. The dual-mode sorption model, used to describe a sorption isotherm for a single penetrant species in a glassy polymer, is discussed elsewhere[24]. The ideal permselectivity of a polymer film for gas A over gas B is given by:

$$\alpha^* = P_A/P_B \tag{4}$$

where $P_A$ and $P_B$ are the pure-gas permeability coefficients of gases A and B. Instead of the permeability coefficient $P$, a pressure-normalized gas flux $(P/l)$ is sometimes used, if the thickness $l$ of the given film is not known. The ideal selectivity can be factorized into a solubility selectivity and a diffusivity selectivity by substituting equation (3) in equation (4):

$$\alpha^* = \left(\frac{D_A}{D_B}\right)\left(\frac{S_A}{S_B}\right) \tag{5}$$

The diffusivity selectivity reflects the ability of the polymer matrix to discriminate between gas molecules on the basis of their size and shape. Factors influencing this selectivity are segmental mobility and intersegmental

packing of the polymer chains. The solubility selectivity from single-gas measurements depends on the level of solubility for the given gases in the polymer matrix and on the free volume available for sorption.

It is clear from equation (5) that only a combination of the solubility selectivity and the diffusivity selectivity can be observed by separate permeation measurements for two single gases. Helium was chosen as a reference gas for the time-dependent permeation measurements made here, since it has a very low solubility in polymers. However, its permeability is very high, compared to $N_2$ and $O_2$, owing to the small size of the helium atom. If the densification of a glassy polymer by physical ageing is to be observed, it is advantageous to choose a gas pair such as He and $N_2$, since minimal effect is expected on the He permeability, but a significant decrease in the $N_2$ permeability will cause a large and easily observed increase in the ideal $He/N_2$ selectivity.

The activation energy of permeation $E_p$ for a single gas in the absence of significant plasticization can be calculated from the slope of an Arrhenius plot of the permeabilities $P$ or normalized fluxes $(P/l)$ as a function of inverse temperature[25]:

$$P = P_0 \exp(-E_p/RT) \tag{6}$$

with $R$ being the gas constant, $T$ the temperature (K), $E_p$ the activation energy of permeation (kcal mol$^{-1}$) and $P_0$ the pre-exponential factor. The activation energy of permeation can be expressed as:

$$E_p = E_D + \Delta H_S \tag{7}$$

where $E_D$ is the activation energy of diffusion and $\Delta H_S$ is the enthalpy of sorption. $E_D$ can be related to the cohesive energy density ($CED$) approximately by[26]:

$$E_D = (CED)d^2\pi(\lambda/4) \tag{8}$$

where $d$ is the radius of a diffusing molecule and $\lambda$ is the length of an idealized cylindrical cavity needed to execute a diffusive jump of the molecule. To interpret differences in $E_p$, which we have detected for glassy polymer films of different thicknesses, it is necessary to take the effects of ageing on both $E_D$ and $\Delta H_S$ into account. The sorption capacity in glassy polymers below $T_g$ decreases upon annealing owing to a decrease in the Langmuir sorption component of the dual-mode model[27].

The contribution of $\Delta H_S$ is negative (heat evolved) below $T_g$ and positive (or, in some cases, less negative) above $T_g$ (ref. 26). This is due to the existence of molecular-scale holes in glasses below $T_g$. If physical ageing below $T_g$ leads to a decrease of the number of pre-existing sorption sites, $E_p$ is expected to increase. Physical ageing and the concurrent densification will also increase the activation energy of diffusion, since the cohesive energy density is expected to increase.

## EXPERIMENTAL

### *Materials*

The polyimide 6FDA–IPDA represents an attractive polymer for membrane gas separations[28]. It is polymerized from hexafluorodianhydride (6FDA) and isopropylidenedianiline (IPDA)[29]. The repeat unit is shown in *Figure 1a*. The polymer was synthesized by Boron Biologicals (Raleigh, North Carolina). The polysulfone used here is a commercial grade (Udel P 1700 NT11, Amoco, Ridgefield, Connecticut). The repeat unit is shown in *Figure 1b*. Some physical and gas transport data are shown in *Table 1*.

All films were cast from solutions of the polymers in methylene chloride (Mallinckrodt, reagent grade) using the same batches of the two polymers. The polymers and the solvent were used without further purification.

### *Film thickness and preparation*

In this work, films are designated as thick ($\sim$1 mil = 25.4 $\mu$m = 254 000 Å), intermediate ($\sim$25 000 Å = 2.5 $\mu$m) and thin ($\sim$0.5 $\mu$m = 5000 Å). Polymer solution was cast into stainless-steel rings (inner diameter 104 mm, height 15 mm) on a levelled mirror glass plate using a glass syringe. A Teflon filter (Cole-Parmer, 0.2 $\mu$m pore size) was attached to the syringe and the solution was filtered directly into the casting ring. Solvent evaporation was slowed by covering the casting rings immediately.

Thick films were cast from solutions containing about 3 wt% of polymer. The amount of solution per film was 5 to 8 cm$^3$. The films were released from the glass plate with deionized water. Intermediate and thin films were then transferred onto the surface of a deep water bath (deionized water) by floating the thin films from the glass plate on a wet filter paper and then immersing this filter paper in the bath. The films were taken up on wire rings

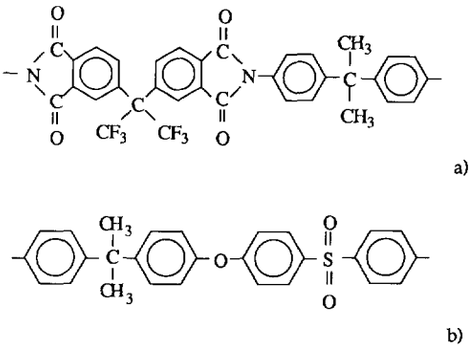


**Figure 1** Repeat units of (a) 6FDA–IPDA polyimide and (b) polysulfone

**Table 1** Some physical and gas transport data at 35°C for 6FDA–IPDA polyimide[30] and Udel 1700 polysulfone[31]

| | Permeability, $P$ (Barrer)[a] | | | | $d$-spacing (Å) | Density (g cm$^{-3}$) | $T_d$ (°C) | $T_g$ (°C) |
|---|---|---|---|---|---|---|---|---|
| | $N_2$ | $O_2$ | He | $CO_2$ | | | | |
| Polyimide | 1.33 | 7.53 | 71.2 | 30.0 | 5.71 | 1.352 | 480 | 310 |
| Polysulfone | 0.25 | 1.4 | 13.0 | 5.6 | 5.0 | 1.240 | – | 186 |

[a] 1 Barrer = $10^{-10}$ cm$^3$(STP) cm/cm$^2$ cmHg s

for preliminary drying in ambient air. *Figure 2* shows the procedures schematically. Somewhat similar techniques have been reported[32-34]. With our technique, the polymer film is obtained free and not attached to the surface of a substrate.

Thick films were measured with a mechanical thickness gauge (Mitutoyo Digimatic, resolution $5 \times 10^{-5}$ inch ($\sim 1.25\ \mu m$)), after drying (see below). Then, thin and intermediate films were cast by simply diluting the solution used for the thick films proportionately with solvent. About 5 $cm^3$ was maintained as the total casting volume per film. A nominal thickness on the basis of a mass balance can then be assigned assuming that the density of thin films does not differ greatly from that of thick films.

For the work presented here, all intermediate and thin films will be identified by their 'nominal thickness' determined from the simple mass-balance considerations given above. Scanning electron micrographs of thin films showed that the thickness estimate by mass balance was reasonably accurate.

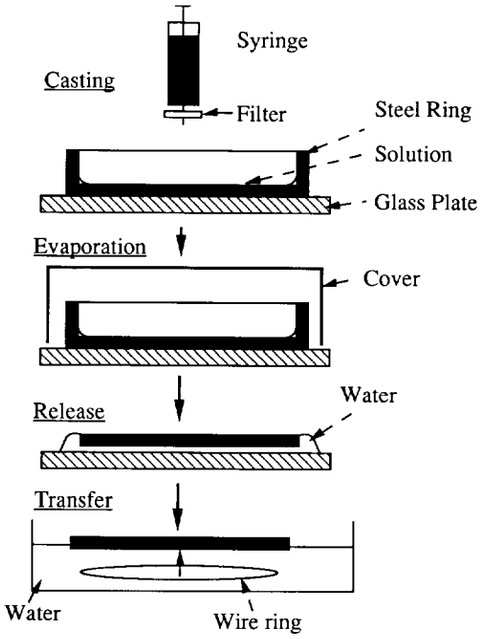


**Figure 2** Casting and release of polymer films

*Drying and thermal history*

It is extremely important to use a consistent and well defined procedure for drying and thermal treatment of glassy polymer samples to remove any doubts about the cause for differences in the film properties[35].

A stainless-steel sample chamber is placed inside of the programmable oven of a Hewlett-Packard 5880A Gas Chromatograph (g.c.). A helium stream is purged continuously through a pre-heating coil into the sample chamber (chamber 180 $cm^3$, purge 10 $cm^3$(STP)/s). The film sample rests freely on a Teflon O-ring supported by a stainless-steel frame. The advantages of this technique are:

(1) No contamination from vacuum pumps or chemicals.
(2) Residual solvent vapour pressure can be easily lowered to zero.
(3) Well defined sample temperature.
(4) Surface orientation owing to contact with solids is reduced.
(5) No reactive gases are present.

The steps for drying and imprinting of a reproducible thermal history are:

(1) Sub-$T_g$ drying for extended times to remove solvents.
(2) Heating with a defined rate to a temperature above $T_g$.
(3) Holding above $T_g$ to erase thermal history, relieve stresses and remove orientation.
(4) Controlled quenching to room temperature.

*Figure 3* shows the drying/quenching programmes. A thermocouple was sandwiched between polymer films to measure the actual sample temperature. The reproducibility of this technique was excellent. The quenching rate at $T_g$ was 3.2°C $min^{-1}$ for the polyimide and 3.4°C $min^{-1}$ for polysulfone.

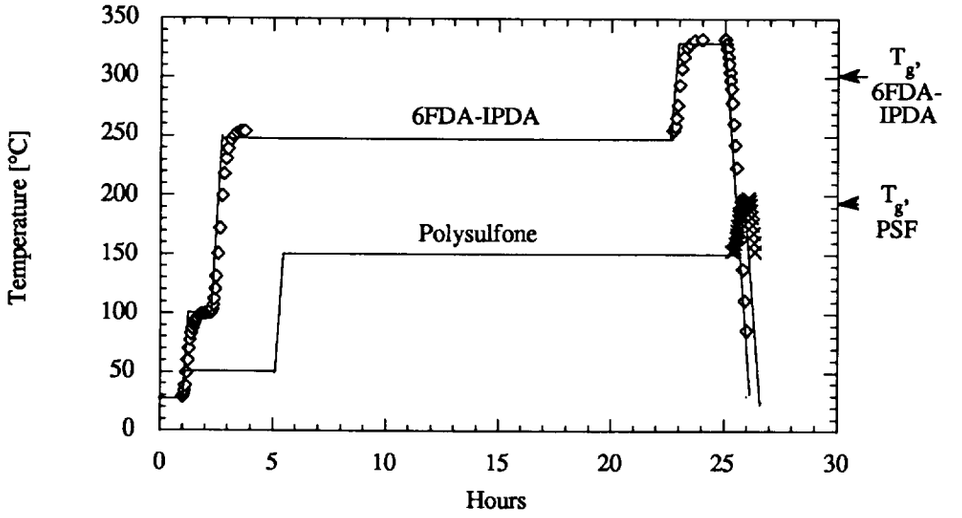


**Figure 3** Drying/quenching procedure. All ramps are 5°C $min^{-1}$. Lines, oven chamber; symbols, polymer films

The likelihood of residual solvent after sub-$T_g$ drying and heating above $T_g$ is quite small, if the maximum film thicknesses and diffusion coefficients for solvents available from the literature are considered[36]. Nevertheless, thick polyimide and polysulfone films were treated with the standard procedure described above, cut into strips ($\sim$5 mm width) and investigated by headspace gas chromatography (h.s.g.c.). These strips were immediately sealed in h.s.g.c. vials ($\sim$0.5 g per vial). Cutting the samples supplied fresh surfaces for the possible diffusion of residual solvent from the samples.

The vials were first stored in an oven at 60°C for three days. Control experiments showed no weight loss of the vials. After storage, the gas phase was analysed using a Hewlett-Packard h.s.g.c. system[37]. No methylene chloride peaks were observed for polysulfone or polyimide samples.

In this work, thin samples were found to show time-dependent properties, while intermediate and thick samples did not. Since the h.s.g.c. experiments were performed on thick films, and the solvent diffusion under dilute conditions can be assumed to scale with the square of the sample thickness, it is clear that the time-dependent properties of thin samples are not caused by removal of residual solvent.

*Permeation measurements*

Single-gas permeation measurements were performed in a constant-volume/variable-pressure apparatus[38]. Besides the usual mounting techniques for thick and intermediate films[38], a special method was employed for thin films. A porous filter (MSI, Westboro, Massachusetts; nylon, 0.1 $\mu$m nominal pore size, Cat. No. N01SP04700) or a ceramic filter (Anopore, 200 Å pore size[39]) was used to support the thin films in a commercially available Millipore test cell. The film was placed on the support in the permeation cell with a partial vacuum applied to the permeate side to hold the film in place. The permeation area was then masked off with heavy-duty aluminium foil with a pre-cut opening. The aluminium foil was then sealed around the edge of the opening with a thin bead of quick-setting epoxy adhesive. Ambient air was circulated over the open test cell. The cell was closed after 20 to 30 min of curing time and an $N_2$ purge stream was applied at atmospheric pressure for at least 24 h. Control experiments with intermediate films on either of the supports showed no influence of the support on the results.

In control experiments with aluminium foil sealing the cell completely, the outgassing of the support materials was observed and the leak rate of the permeate system was determined. It was found that after one day of evacuation, outgassing had subsided to levels below the detectability limit, which is given by the leak rate of the permeate system ($<10^{-3}$ Torr h$^{-1}$, permeate volume 1200 cm$^3$).

All gases used were at least 99.99% pure. In all permeation experiments, a small purge stream was maintained across the feed side of the membrane ($\sim$5 cm$^3$(STP)/min), to avoid any accumulation of impurities during extended tests. A liquid-nitrogen trap or an adsorbent trap was always used to prevent any back-diffusion of vacuum-pump oils.

The permeation area of thick and intermediate films was always about 5 cm$^2$. Smaller areas were masked off for thin films. This was necessary to avoid defects and creases visible in the thin films.

The masked permeation areas were determined by successive magnified photocopies taken after the end of the experiments. The permeation area was clearly visible. The image of the permeation area was cut out and weighed. By inclusion of a scale bar, the permeation area could be calculated. To determine the accuracy of this method, a circular metal disc with an actual area of 3.5442 cm$^2$ (mechanical gauge, resolution $5\times10^{-5}$ inch ($\sim$1.25 $\mu$m)) was used to verify the procedure. The average area determined by the above procedure was 3.5647 cm$^2$ (five independent measurements, standard deviation 0.0485 = 1.4%).

It should be kept in mind that any small errors in the permeation area of the films only have an influence on the absolute values of the permeabilities, but not on selectivities, activation energies of permeation, or qualitative time dependences.

The time-dependent permeation measurements were performed at 35°C and 150 psia ($\sim$1035 kPa). Gas exchanges were performed without depressurization. Purging of the feed system for a gas exchange is described in detail elsewhere[40].

*Activation energies of permeation*

The activation energies of permeation $E_p$ for $N_2$, $O_2$ and He were determined by steady-state permeation measurements at 20, 35 and 50°C. A linear regression was then used to determine the slope $E_p$ of a plot of ln $P$ *versus* $1/T$ according to:

$$\ln P = \ln P_0 + (E_p/R)\times(1000/T) \qquad (9)$$

where $P$ is the permeability for the given gas at the temperature $T$, $P_0$ is a reference permeability and $R$ is the gas constant. The uncertainty of this method has been estimated[41] to be $\pm$0.2 kcal mol$^{-1}$.

## RESULTS AND DISCUSSION

*Time-dependent permeation measurements*

The time of quenching through the glass transition temperature was used as time zero. Samples that were only air dried after casting pass through the glass transition while the solvent evaporates from the film. The reference time for air-dried samples was chosen as the time of casting. An air-dried thin sample is included in the results to show that the usual drying procedure is not responsible for time-dependent behaviour of thin films.

The general test programme is shown in *Figure 4*. Also shown is the type of information to be derived from each part of the test sequence. Time-dependent $N_2$ permeabilities for polyimide 6FDA–IPDA films are shown in *Figure 5*. The thick film clearly ages somewhat. This has been previously observed[30]. The intermediate film shows very similar behaviour.

Data for two thin films are shown in *Figure 5*, and both exhibit much lower permeabilities with a significant time dependence. Ageing persists through periods of storage without applied gas pressure (see arrows). One of the thin films has only been dried at room temperature in air and its shows ageing similar to the 'standard dried' thin film. *Figure 6* shows the ideal He/$N_2$ selectivities corresponding to *Figure 5*. Both thin films show a strong

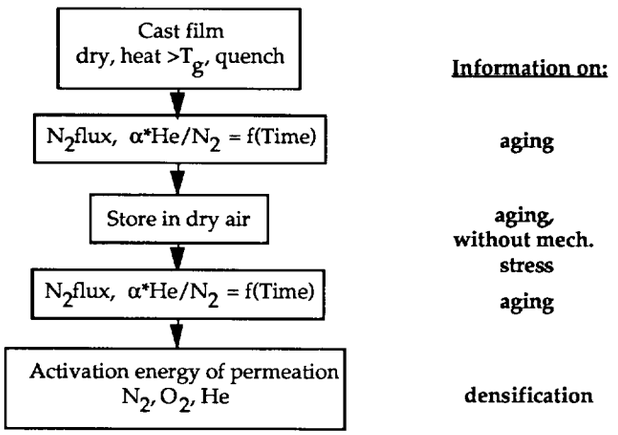


**Figure 4** Drying/test programme to determine time-dependent gas permeation properties

increase of the ideal He/$N_2$ selectivity with time, far above the thick and intermediate film values. Storage at atmospheric pressure (arrows) appears to accelerate ageing slightly. Defects, if they were present, would be most likely found in the thin films and would be expected to lower the selectivities below thick-film values. The opposite is found here.

The continued increase of the selectivity through the timespan of storage without applied gas pressure confirms that mechanical stress is not the cause. The absolute values of the selectivities are not dependent on measurements of film thickness or area and therefore offer an excellent measure of the physical ageing process.

The magnitude and time dependence of the selectivities give striking evidence that the physical ageing process is accelerated in thin films. However, the time dependence and increased selectivity nearly vanish on increasing the film thickness by only a factor of about 5 from 5000 Å

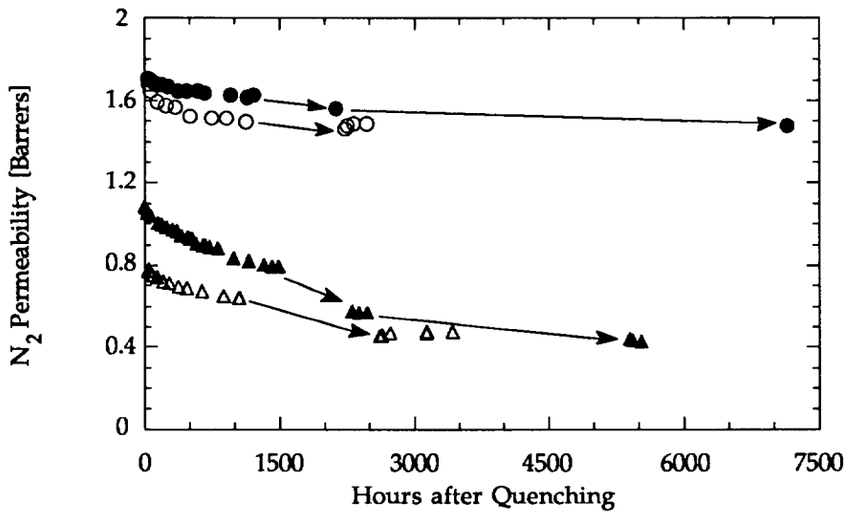


**Figure 5** $N_2$ permeability of 6FDA–IPDA polyimide films (35°C, 150 psia): (●) thick, 28.45 μm; (○) intermediate, 2.54 μm; (△) thin, 0.5 μm = 5000 Å; (▲) thin, air dried at RT only. Arrows: storage, 35°C, 1 atm, in dry air

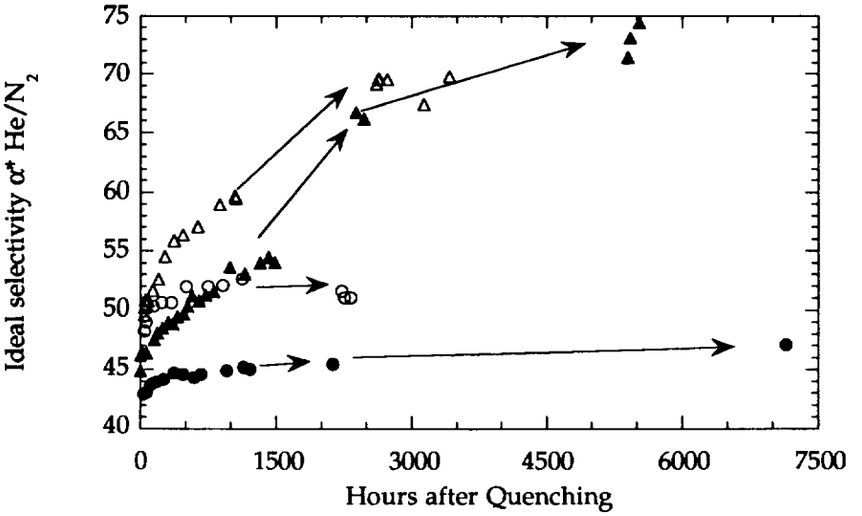


**Figure 6** Ideal selectivity α*($He/N_2$) of 6FDA–IPDA polyimide films (35°C, 150 psia): (●) thick, 28.45 μm; (○) intermediate, 2.54 μm; (△) thin, 0.5 μm = 5000 Å; (▲) thin, air dried at RT only. Arrows: storage, 35°C, 1 atm, in dry air

to 25 400 Å. This points to a strong dependence of ageing on the film thickness.

Similar time-dependent selectivities for the same polyimide have been observed for ultrathin asymmetric and composite membranes[11,15]. The final values far exceeded thick-film values and are comparable to the values reported here. Only speculations on the causes for these observations were possible, since the thermal and mechanical histories of these membranes are not well defined and are quite different from those of thick films. The evidence shown here for 6FDA–IPDA polyimide films that are virtually identical, except for their thickness, points clearly to accelerated physical ageing in thin films as the underlying cause.

Similar experiments were performed for polysulfone. *Figure 7* shows the $N_2$ permeabilities for polysulfone films. *Figure 8* shows the ideal $He/N_2$ selectivities. The intermediate and thick films show virtually constant properties, with a slightly increased selectivity and lower permeability for the intermediate film. The thin polysulfone film shown in *Figures 7* and *8* was only stored in dry air and never pressurized, until the first data points shown. The increased selectivity and decreased permeability show again that accelerated ageing takes place in the thin films with or without the mechanical stress of the applied gas pressure. The results are qualitatively very similar to the polyimide results.

### *Activation energies of permeation*

The activation energies of permeation ($E_p$) for $N_2$, $O_2$ and He are shown in *Figure 9* for thick, intermediate and thin films of polyimide 6FDA–IPDA. The films had been previously used in the permeation experiments described above. The stable permeabilities and selectivities of thick and intermediate films before the $E_p$ measurements were

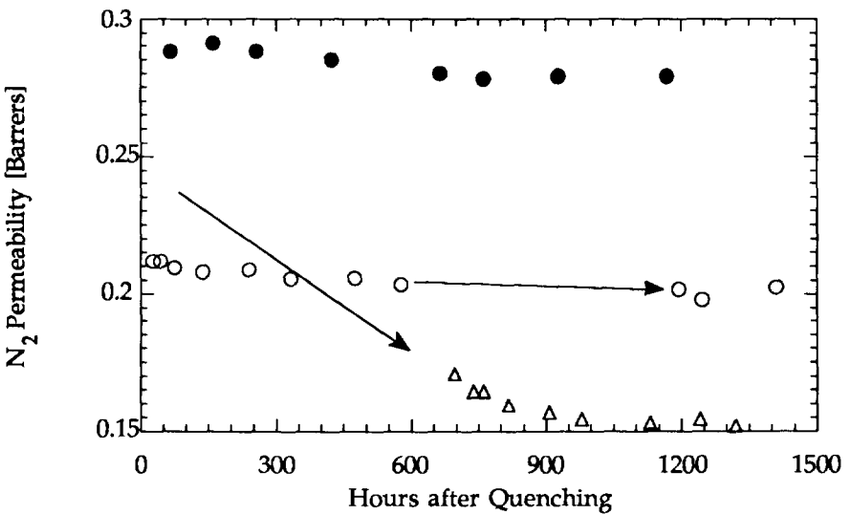


**Figure 7** $N_2$ permeability of polysulfone films (35°C, 150 psia): (●) thick, 23.88 μm; (○) intermediate, 2.54 μm; (△) thin, 0.5 μm = 5000 Å. Arrows: storage, 35°C, 1 atm, in dry air

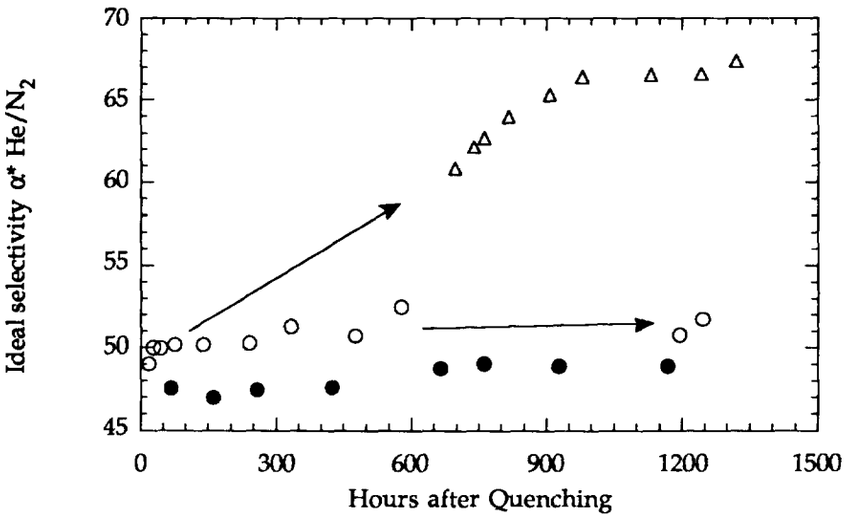


**Figure 8** Ideal selectivity $\alpha^*(He/N_2)$ of polysulfone films (35°C, 150 psia): (●) thick, 23.88 μm; (○) intermediate, 2.54 μm; (△) thin, 0.5 μm = 5000 Å. Arrows: storage, 35°C, 1 atm, in dry air

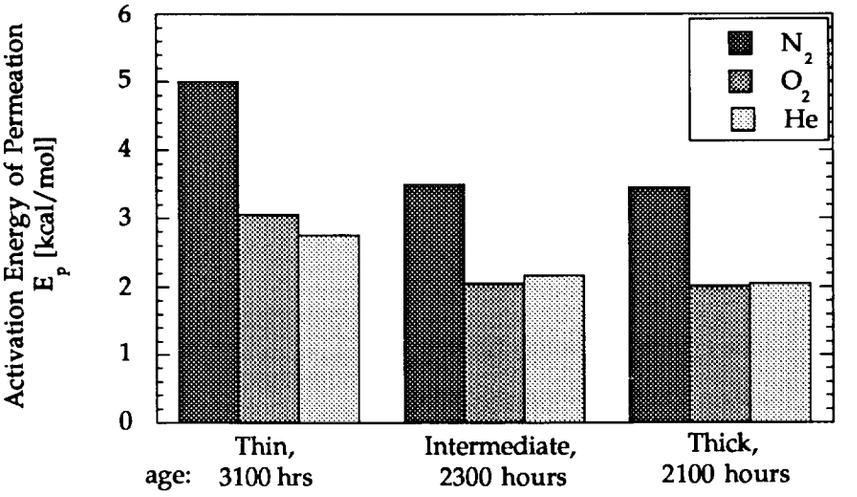


**Figure 9** Activation energies of permeation for thin, intermediate and thick films from 6FDA–IPDA polyimide (150 psia, 20–50°C)

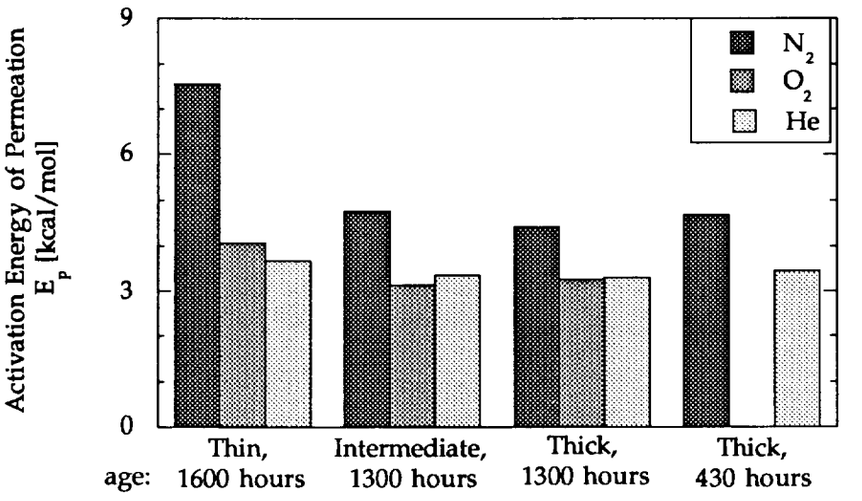


**Figure 10** Activation energies of permeation for thin, intermediate and thick films from polysulfone (150 psia, 20–50°C)

taken as an indication that no further ageing was apparent on this timescale.

The thin film shows clearly increased activation energies while the intermediate and thick films show lower and very similar activation energies. Thickness differences of a factor of about 10, from the thick film to the intermediate film, apparently do not cause significant changes. These results agree with the behaviour of gas selectivities and permeabilities found for thick and intermediate films. Accelerated physical ageing of the thin films appears to be a likely explanation for the increased $E_p$ values. The thick and intermediate films do not reach this level of densification.

Using the maximum difference in $E_p$ for $N_2$ between the aged thin film and the thick film, one can estimate the increase in the cohesive energy density ($CED$) that would be needed to cause this increase in $E_p$. The assumption that the increase in $E_p$ is mainly due to an increase in $E_D$ is made and the result should only be used as a plausibility check of the $E_p$ data. This estimation yields:

$$\Delta(CED)_{\text{thin/thick}} \approx E_{p,\text{thin}} - E_{p,\text{thick}} = 1.68 \text{ kcal mol}^{-1} \quad (10)$$

Using a bulk density for 6FDA–IPDA polyimide of 1.352 g cm$^{-3}$ and a molecular weight per repeat unit of 634 g mol$^{-1}$, a value of 14.99 J cm$^{-3}$ is found for $\Delta(CED)_{\text{thin/thick}}$. Values for the $CED$ of polymers[42] are in the range of several hundred J cm$^{-3}$. Therefore, the observed change in $CED$ by densification does not seem unreasonable.

The results for the $E_p$ values of polysulfone give a very similar picture. *Figure 10* shows the clearly increased activation energies for the thin polysulfone film, when compared to thick and intermediate films. The conclusions for the results with polysulfone are similar to the polyimide results. Thickness-dependent ageing appears to densify the polymer matrix in the thin film, which causes increased $E_p$ values, increased ideal gas selectivities and concurrently decreased permeabilities.

## CONCLUSIONS

Thin glassy polymer films show significant evidence of accelerated physical ageing deep in the glassy state, while thick and intermediate films from the *same material* and with *identical history* show no such effects over the observed times. The decreasing gas permeabilities, increased selectivities and other anomalies that have been detected elsewhere for ultrathin gas separation membranes can be rationalized in relation to accelerated ageing of thin glassy polymer films.

## ACKNOWLEDGEMENTS

The authors acknowledge the financial support of the Department of Energy, Basic Energy Sciences Program, and the Texas Advanced Technology Program (ATP035).

## REFERENCES

1 Stannett, V. T., Koros, W. J., Paul, D. R., Lonsdale, H. K. and Baker, R. W. in 'Advances in Polymer Science', Vol. 32, Springer-Verlag, Berlin, 1979
2 Stookey, D. J., Patton, C. J. and Malcolm, G. L. *Chem. Eng. Prog.* Nov. 1986, p. 36
3 Koros, W. J. and Chern, R. T. in 'Handbook of Separation Process Technology' (Ed. R. W. Rousseau), Wiley, New York, 1987, p. 862
4 Struik, L. C. E. 'Physical Aging in Amorphous Polymers and Other Materials', Elsevier, New York, 1978
6 Kovacs, A. J. *J. Polym. Sci.* 1958, **30**, 131
7 Braun, G. and Kovacs, A. J. *Phys. Chem. Glasses* 1963, **4**, 152
8 Berens, A. R. and Hopfenberg, H. B. *J. Polym. Sci. (B) Polym. Phys.* 1979, **17**, 1757
9 Berens, A. R. and Hopfenberg, H. B. *Polymer* 1978, **19**, 489
10 Enscore, D. J., Hopfenberg, H. B., Stannett, V. T. and Berens, A. R. *Polymer* 1977, **18**, 1105
11 Pinnau, I., Hellums, M. W. and Koros, W. J. *Polymer* 1991, **32**, 2612
12 Pinnau, I. PhD Dissertation, University of Texas at Austin, 1991
13 Pfromm, P. H., Pinnau, I. and Koros, W. J. *J. Appl. Polym. Sci.* 1993, **48**, 2161
14 Pfromm, P. H., Pinnau, I. and Koros, W. J. Topical Conference on Separations Technologies, AIChE Preprints Paper Number 25b, Miami, FL, 1992
15 Rezac, M. E., Pfromm, P. H., Costello, L. M. and Koros, W. J. *Ind. Eng. Chem. Res.* 1993, **32**, 1921
16 Alfrey, T., Goldfinger, G. and Mark, H. *J. Appl. Phys.* 1943, **14**, 700
17 Bogdanova, L. M., Ponomareva, T. I., Irzhak, V. I. and Rozenberg, B. A. *Polym. Sci. USSR* 1984, **26**, 1566
18 Pucalka, V. *Thin Solid Films* 1967/68, **1**, 429
19 Mader, S. *Thin Solid Films* 1976, **35**, 195
20 Mader, S. and Herd, S. *Thin Solid Films* 1972, **10**, 377
21 Spaepen, F. *J. Non-Cryst. Solids* 1978, **31**, 207
22 von Wroblewski, S. *Ann. Physik* 1879, **8**, 29
23 Vieth, W. R., Howell, J. M. and Hsieh, J. H. *J. Membr. Sci.* 1976, **1**, 177
24 Barrer, R. M., Barrie, J. A. and Slater, J. *J. Polym. Sci.* 1958, **27**, 177
25 Stannett, V. in 'Diffusion in Polymers' (Eds J. Crank and G. S. Park), Academic Press, New York, 1968, Ch. 2
26 Meares, P. *J. Am. Chem. Soc.* 1954, **76**, 3415
27 Chan, A. H. and Paul, D. R. *Polym. Eng. Sci.* 1980, **20**, 87
28 Kim, T.-H., Koros, W. J., Husk, G. R. and O'Brien, K. C. *J. Membr. Sci.* 1988, **37**, 45
29 Husk, G. R., Cassidy, P. E. and Gebert, K. L. *Macromolecules* 1988, **21**, 1234
30 Kim, T.-H. PhD Dissertation, University of Texas at Austin, 1988
31 McHattie, J. S. PhD Dissertation, University of Texas at Austin, 1990
32 Riley, R. L., Lonsdale, H. K., Lyons, D. R. and Merten, U. *J. Appl. Polym. Sci.* 1967, **11**, 2143
33 Carnell, P. H. *J. Appl. Polym. Sci.* 1965, **9**, 1863
34 Carnell, P. H. and Cassidy, H. G. *J. Polym. Sci.* 1961, **55**, 233
35 Vrentas, J. S. and Hou, A.-C. *J. Appl. Polym. Sci.* 1988, **36**, 1933
36 Berens, A. R. and Hopfenberg, H. B. *J. Membr. Sci.* 1982, **10**, 283
37 Simpson, E. and Pfromm, P. H., to be published
38 Koros, W. J. PhD Dissertation, University of Texas at Austin, 1977
39 Furneaux, R. C., Rigby, W. R. and Davidson, A. P. *Nature* 1989, **337**, 147
40 Pfromm, P. H. PhD Dissertation, University of Texas at Austin, 1994
41 Costello, L. M. and Koros, W. J. *Ind. Eng. Chem. Res.* 1992, **31**, 2708
42 Pace, R. J. and Datyner, A. *Polym. Eng. Sci.* 1980, **20**, 51